Detection of Reduced Retinal Vessel Density in Eyes with Geographic Atrophy Secondary to Age-Related Macular Degeneration Using Projection-Resolved Optical Coherence Tomography Angiography

QI SHENG YOU, JIE WANG, YUKUN GUO, CHRISTINA J. FLAXEL, THOMAS S. HWANG, DAVID HUANG, YALI JIA, AND STEVEN T. BAILEY

• PURPOSE: To compare retinal vessel density in eyes with geographic atrophy (GA) secondary to age-related macular degeneration (AMD) to age-matched healthy eyes by using projection-resolved optical coherence tomography angiography (PR-OCTA).
• DESIGN: Prospective cross-sectional study.
• METHODS: Study participants underwent macular 3- × 3-mm OCTA scans with spectral domain OCTA. Reflectance-compensated retinal vessel densities were calculated on projection-resolved superficial vascular complex (SVC), intermediate capillary plexus (ICP), and deep capillary plexus (DCP). Quantitative analysis using normalized deviation compared the retinal vessel density in GA regions, 500-μm GA rim regions, and non-GA regions to similar macular locations in control eyes.
• RESULTS: Ten eyes with GA and 10 control eyes were studied. Eyes with GA had significantly lower vessel density in the SVC (54.8 ± 2.4% vs. 60.8 ± 3.1%; $P < 0.001$), ICP (34.0 ± 1.5% vs. 37.3 ± 1.7%; $P = 0.003$) and DCP (24.4 ± 2.3% vs. 28.0 ± 2.3%; $P < 0.001$) than control eyes. Retinal vessel density within the GA region decreased significantly in SVC, ICP, and DCP. Retinal vessel density in the GA rim region decreased in SVC and ICP but not in DCP. The non-GA region did not significantly deviate from normal controls. Eyes with GA had significantly reduced photoreceptor layer thickness; but similar nerve fiber layer, ganglion cell complex, inner nuclear layer, and outer plexiform layer thickness.
• CONCLUSIONS: Eyes with GA have reduced retinal vessel density in SVC, ICP, and DCP compared to those in controls. Loss is greatest within regions of GA. Vessel density may be more sensitive than retinal layer thickness measurement in the detection of inner retinal change in eyes with GA. (Am J Ophthalmol 2020;209:206–212. © 2019 Elsevier Inc. All rights reserved.)

Accepted for publication Sep 10, 2019.

From the Casey Eye Institute (Q.S.Y., Y.G., C.J.F., T.S.H., D.H., Y.J., S.T.B.), Oregon Health and Science University, Portland, Oregon, USA; and the Department of Biomedical Engineering (J.W., Y.J.), Oregon Health and Science University, Portland, Oregon, USA.

Inquiries to Steven T. Bailey, Casey Eye Institute, Oregon Health and Science University, 3375 SW Terwilliger Boulevard, Portland, Oregon 97239; e-mail: bailstev@ohsu.edu

ADVANCED AGE-RELATED MACULAR DEGENERATION (AMD), in its neovascular and atrophic forms, is the leading cause of vision loss, particularly in industrialized countries.[1–3] Geographic atrophy (GA) causes a slow irreversible vision loss, accounting for approximately 20% of all cases of legal blindness in North America.[4] With the advent and success of antivascular endothelial growth factor for the treatment of neovascular AMD,[5–7] GA could become the leading cause of severe vision loss in the future.

GA is clinically characterized by sharply demarcated atrophic lesions of the outer retina and retinal pigment epithelium (RPE) with an increased visibility of underlying choroidal vessels.[4] Although GA affects primarily the outer retina, with loss of photoreceptors, RPE and the choriocapillaris, improved knowledge of inner retinal status in GA may be relevant for understanding the disease and developing potential therapies such as retinal prosthesis or stem cell therapy. Studies have previously demonstrated inner nuclear layer and ganglion cell loss in addition to outer retinal loss.[8,9] To the best of the present authors' knowledge, there has been no study quantifying changes in inner retinal blood flow in GA. Considering the secondary loss of inner retinal neurons, as shown by previous studies,[9,10] hypothetically there may be changes in perfusion in both the superficial and the deep layer capillaries. Optical coherence tomography angiography (OCTA) provides an opportunity to quantify retinal perfusion noninvasively. However, conventional OCTA has limited vascular depth discrimination due to projection artifacts of superficial flow signal onto deeper layers.[11] The projection-resolved OCTA (PR-OCTA), developed by the present authors' group,[12,13] improves vascular depth resolution by removing projection artifacts while retaining in situ flow signal from real blood vessels

0002-9394/$36.00
https://doi.org/10.1016/j.ajo.2019.09.004

in deeper layers. PR-OCTA enables the observer to study the retinal vasculature within individual plexi in vivo, which was not previously possible.[12,14] The purpose of the current study was to evaluate inner retinal vessel density in the 3 retinal plexi by using PR-OCTA in eyes with GA.

METHODS

THIS PROSPECTIVE CLINICAL OBSERVATIONAL STUDY adhered to the tenets of the Declaration of Helsinki and was conducted in compliance with the Health Insurance Portability and Accountability Act. The institutional review board at Oregon Health and Science University approved the study, and written informed consent was obtained from each participant.

The criteria for GA patient inclusion were age of 50+ years and diagnosis of GA secondary to AMD in at least 1 eye. GA was defined as sharply demarcated atrophic lesions of at least 175 μm with increased visibility of choroidal vessels. The diagnosis of GA was confirmed by both hypoautofluorescence on fundus autofluorescence (FAF) imaging and on OCT scans (Spectralis, Heidelberg, Germany) demonstrating congruent loss of photoreceptors and RPE and hypertransmission of OCT signal into the choroid. A group of age-matched healthy participants was included as control subjects. The criteria for controls inclusion were an age of at least 50 years old, no history of retinal diseases, corrected visual acuity ≥20/20, IOP (IOP) <21 mm Hg and the absence of any abnormalities on clinical fundus examination and OCT. The exclusion criteria for both GA and control groups included a history of diabetes mellitus, choroidal or retinal neovascularization, previous intraocular surgery except for cataract surgery, any other macular disease such as epiretinal membrane or vitreomacular traction syndrome, refractive error greater than −6 or +3 diopters and media opacities that precluded a high-quality OCTA scan.

All participants underwent a comprehensive ocular examination, including early treatment of diabetic retinopathy study (ETDRS) visual acuity testing, IOP, axial length measurement (IOL master 500, Carl Zeiss Meditec, Dublin, California), dilated fundus examination, fundus photography (model FF450 plus, Carl Zeiss Meditec), OCTA, FAF (Spectralis HRA+OCT; Heidelberg Engineering, Heidelberg, Germany), structural OCT, as well as a systemic blood pressure measurement. The mean arterial pressure (MAP) was calculated as the diastolic blood pressure plus one-third of the difference between the diastolic blood pressure and the systolic blood pressure. The ocular perfusion pressure was determined by subtracting the IOP from the two-thirds of MAP.

OCTA was obtained after pupil dilation by using a commercially available spectral-domain instrument (RTVue XR Avanti; Optovue, Inc., Fremont, California), with a center wavelength of 840 nm and an axial scan rate of 70 kHz. The 3- × 3-mm scans centered on the fovea were acquired. The commercial version of a split-spectrum amplitude decorrelation angiography algorithm[15] was used to detect blood flow by comparing consecutive B-scans at the same location. Each scan set consisted of 1 vertical-priority raster and 1 horizontal-priority raster scan. The AngioVue (Phoenix, Arizona) software uses an orthogonal registration algorithm to register the 2 perpendicular raster volumes to produce a merged 3-dimensional (3D) OCT angiogram. The merged volumetric angiograms were then exported for customized processing using COOL-ART software (New York City, New York).[16] Scans were excluded if images were out of focus, significant motion artifacts were detected, or signal strength index was less than 55.

A semiautomated algorithm based on a directional graph search segmented the volumes.[16,17] Segmentations were then reviewed and manually adjusted to ensure accuracy. Retinal layer thickness measurements were defined by the whole retinal layer, from the internal limiting membrane to the inner surface of RPE; and by the whole nerve fiber layer (NFL), from the internal limiting membrane to the outer surface of the NFL; and by the ganglion cell complex (GCC), consisting of both the ganglion cell layer and the inner plexiform layer (IPL), from the outer surface of the NFL to the inner surface of inner nuclear layer (INL); and by the inner nuclear layer, from inner surface of the INL to the outer surface of the INL; and by the outer plexiform layer (OPL), from the outer surface of the INL to the inner surface of the outer nuclear layer (ONL); and by photoreceptor thickness, from the inner surface of the ONL to the inner surface of the RPE. Retinal vessel density was defined as the proportion of vessel area with blood flow over the total area measured. Reflectance-compensated vessel densities were calculated on projection-resolved superficial vascular complex (SVC), intermediate capillary plexus (ICP), and deep capillary plexus (DCP).[12,13,18] The central 0.6-mm diameter area centered on the fovea was excluded to limit the effect of foveal avascular zone on vessel density measurement.[19–22] An en face OCT reflectance map was used to identify areas of GA.

Retinal vessel densities were calculated within GA regions, within the GA rim region (500 μm rim around GA), and in the non-GA regions that included regions outside of the GA rim area.[23] For eyes with multiple GA regions, a mean vessel density of all GA regions or rim area was calculated by dividing the sum of vessel area within GA region or rim area by the total GA area or total rim area. Because GA locations varied among individuals and because vessel density varied by location within the macula,[14] fractional vessel density deviation maps were calculated normalized to the average vessel density map in the normal control group. The normalized vessel deviation was defined as the value from the eye under evaluation minus the normal average and then divided by the normal average. Thus, the reduction of vessel density within GA

TABLE 1. Clinical Characteristics of Study Participants with Geographic Atrophy Secondary to Age-Related Macular Degeneration and Age-Matched Controls

Parameters	Healthy Control (n = 10) Mean ± SD	Ga Patients (n = 10) Mean ± SD	*P* Value
Age, y	76.3 (4.2)	81.3 (9.3)	0.14
Males/females	7/3	7/3	1.00
Axial length, mm	24.62 (0.85)	24.02 (0.63)	0.09
Intraocular pressure, mm Hg	14.8 (2.4)	13.8 (2.8)	0.41
Visual acuity, ETDRS letters	85.7 (2.1)	73.1 (7.0)	<0.001
Systolic blood pressure, mm Hg	126.2 (18.7)	130.2 (18.4)	0.67
Diastolic blood pressure, mm Hg	74.4 (11.1)	74.4 (10.8)	1.00
Ocular perfusion pressure, mm Hg	46.4 (8.2)	48.2 (6.4)	0.59

ETDRS = Early Treatment Diabetic Retinopathy Study; Ga = geographic atrophy; OCTA = optical coherence tomography angiography.

rims could be calculated by averaging the normalized vessel density deviation in the rim area. The analytical areas were centered on the foveal avascular zone and adjusted for transverse optical magnification calculated according to the axial length of each eye. The pixel coordinate was used to match the location when comparing GA region, GA rim, and non-GA region to corresponding areas of normal average maps.

Statistical analysis was conducted using SPSS version 25.0 (IBM, Armonk, New York) for Windows (Microsoft, Redmond, Washington). Descriptive statistics included mean, standard deviation (SD), and range, and percentages were presented where appropriate. The Shapiro-Wilk test was used to test normality of data distribution of age, axial length, retinal layer thickness, and vessel density. An independent sample *t* test was used to compare age, axial length, retinal thickness, and vessel density on each individual plexus between eyes with GA and healthy normal eyes. Pearson correlation was used to analyze the correlation between extent of vessel density reduction and GA size, and the correlation between vessel densities and retinal layer thicknesses. A 1-sample t test was used to determine whether the normalized deviation was significantly different from zero within the GA region and GA rims and outside the GA rim region. All *P* values were 2-sided and considered statistically significant if the value was less than 0.05. Bonferroni correction was applied when doing multiple comparisons.

RESULTS

ONE EYE EACH OF 10 GA PATIENTS (7 WOMEN) AND 10 normal healthy controls (7 women) were included. The mean ages were 81.3 ± 9.3 (range, 66–95 years) and 76.3 ± 4.2 years (range, 73–85 years) for GA and control groups, respectively ($P = 0.14$). The axial length was not significantly different between GA and control eyes (24.02 ± 0.63 mm vs. 24.63 ± 0.85 mm, respectively; $P = 0.09$). The systolic arterial blood pressure, diastolic blood pressure, IOP, and calculated ocular perfusion pressure were similar between the 2 groups. On the 3- × 3-mm OCTA scan area, GA lesion was multifocal in 9 of 10 eyes and monofocal in 1 of 10 eyes. The mean atrophic area was 1.84 ± 1.00 mm^2 (range, 0.72–4.35 mm^2) on 3- × 3-mm en face OCT scans. Table 1 summarizes the clinical characteristics of the participants.

The mean retinal vessel densities were significantly lower in GA eyes than in normal controls in SVC (54.8 ± 2.4% vs. 60.8 ± 3.1%, respectively; $P < 0.001$), ICP (34.0 ± 1.5% vs. 37.3 ± 1.7%, respectively; $P < 0.001$), and DCP (24.4 ± 2.3% vs. 28.0 ± 2.3%, respectively; $P = 0.002$). The DCP in eyes with GA had the greatest reduction (13%) of retinal vessel density compared to the DCP of normal controls, followed by the SVC (10%) and ICP (9%). The GA size was not significantly associated with the extent of vessel density reduction in SVC ($P = 0.24$), ICP ($P = 0.31$), or DCP ($P = 0.59$).

Quantitative analysis using normalized deviation compared the retinal vessel density in GA regions, GA rim regions, and non-GA regions to similar macular locations in control eyes (Table 2). The retinal vessel density within the GA region was significantly lower in SVC, ICP, and DCP. Retinal vessel density in the GA rim region decreased in only the SVC and ICP but not in the DCP. The non-GA region did not deviate from normal controls. The GA region had the greatest reduction in retinal vessel density (Figure).

Compared to normal controls, eyes with GA had significantly reduced whole-retinal layer thickness (254.3 ± 9.6p; vs. 272.4 ± 12.4 μm, respectively; $P = 0.002$) and photoreceptor layer thickness (90.2 ± 12.1 vs. 110.0 ± 10.1 μm, respectively; $P = 0.001$). There were no differences in NFL (26.0 ± 2.8 vs. 24.4 ± 3.3 μm, respectively; $P = 0.23$), GCC (73.9 ± 4.4 vs. 76.3 ± 5.3 μm, respectively; $P = 0.28$), INL (36.5 ± 4.3 vs. 37.5 ± 2.3 μm, respectively; $P = 0.55$), and OPL thickness (27.6 ± 3.5 vs. 24.3 ± 4.7 μm, respectively; $P = 0.09$) (Table 3).

TABLE 2. Retinal Vessel Density in Eyes with Geographic Atrophy and Age-Matched Controls

Layers	VD (SD)% in control eyes (n = 10)	VD (SD)% in GA eyes (n = 10)	*P* Value	Normalized VD Deviation of GA region	*P* Value (Compared to 0)	Normalized VD Deviation of GA Rims	*P* Value (Compared to 0)	Normalized VD Deviation of non-GA Region	*P* Value (Compared to 0)
SVC	60.76 (3.10)	54.80 (2.37)	<0.001	−0.12	0.005	−0.09	0.003	0.03	0.49
ICP	37.29 (1.71)	34.01 (1.53)	<0.001	−0.20	0.001	−0.06	0.01	0.05	0.40
DCP	28.04 (2.26)	24.39 (2.26)	0.002	−0.32	<0.001	0.01	0.83	0.34	0.09

AMD = age-related macular degeneration; DCP = deep capillary plexus; GA = geographic atrophy; ICP = intermediate capillary plexus; SD = standard deviation; SVC = superficial vascular complex; VD = vessel density.

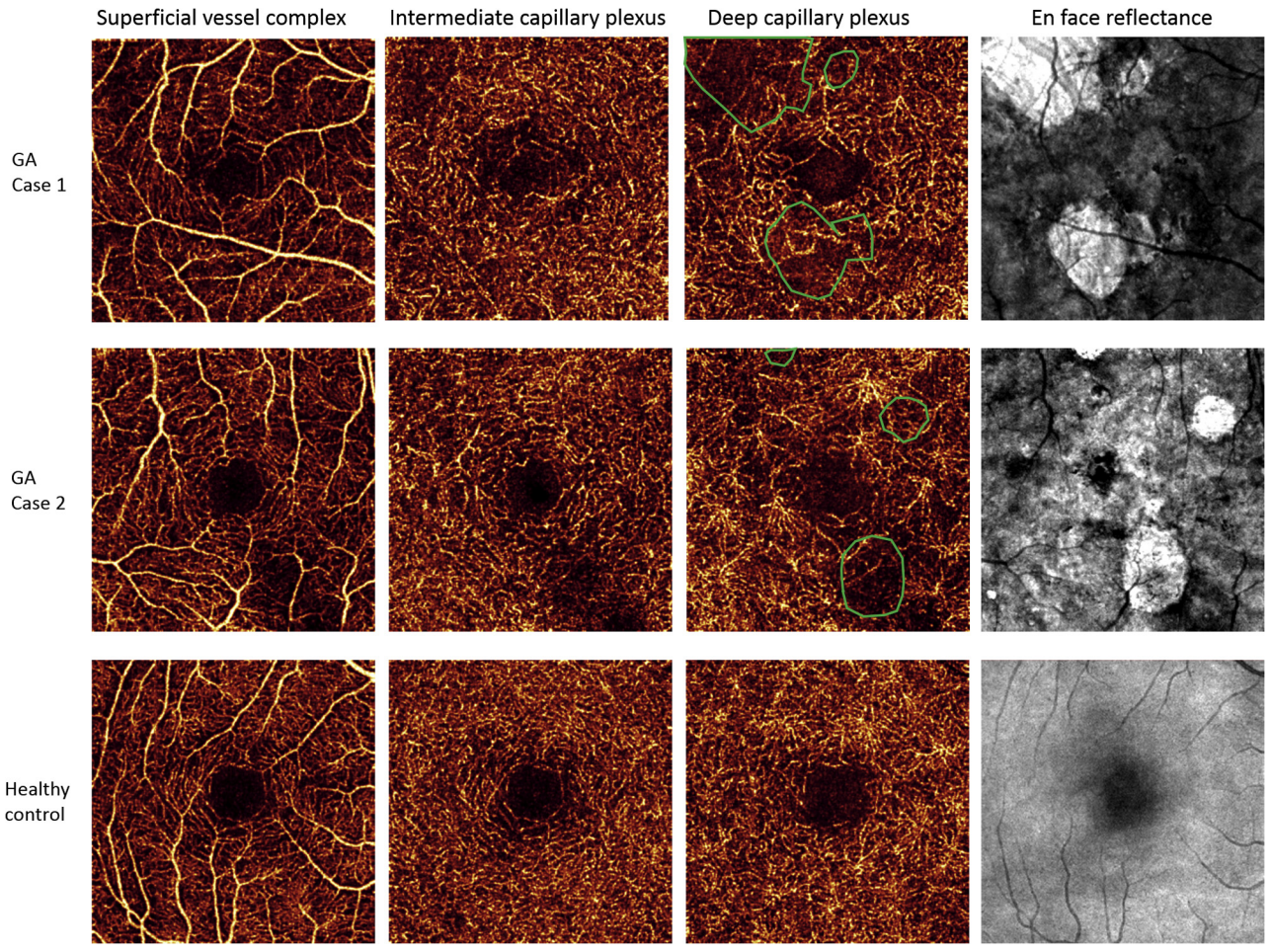

FIGURE. Retinal vessel density is reduced in superficial vessel complex, intermediate capillary plexus, and deep capillary plexus in 2 eyes with geographic atrophy compared to a healthy age-matched control. Retinal vessel density loss was greatest within regions of geographic atrophy (GA) (green outlines).

Quantitative analysis using normalized deviation compared retinal layer thickness in GA regions, GA rim regions, and non-GA regions to similar macular locations in control eyes (Table 3). Within GA regions had significantly reduced photoreceptor layer thickness and reduced all-layer retinal thickness. OPL thickness was increased, and there was no thickness change in NFL, GCC, and INL. Normalized deviation analysis in GA rims demonstrated

TABLE 3. Retinal Layer Thickness in Eyes with Geographic Atrophy and Age-Matched Controls

Retina Layers	Mean ± SD Healthy Control Eyes (μm)	Mean ± SD GA Eyes (μm)	*P* Value	Normalized Deviation of Thickness in GA Region	*P* Value (Compared to 0)	Normalized Deviation of Thickness in GA Rims	*P* Value (Compared to 0)	Normalized Deviation of Thickness in non-GA Region	*P* Value (Compared to 0)
NFL	24.4 (3.2)	26.0 (2.8)	0.23	0.10	0.29	0.04	0.52	0.08	0.18
GCC	76.3 (5.3)	73.9 (4.4)	0.27	0.01	0.79	−0.03	0.17	0.00	0.92
INL	37.5 (2.3)	36.5 (4.3)	0.55	0.002	0.96	−0.05	0.25	−0.02	0.64
OPL	24.3 (4.7)	27.6 (3.5)	0.09	0.22	0.006	0.11	0.06	0.14	0.08
Photoreceptor	110.0 (10.1)	90.2 (12.1)	0.001	−0.64	<0.001	−0.35	<0.001	−0.19	0.03
Whole retina	272.4 (12.4)	254.3 (9.6)	0.002	−0.15	<0.001	−0.08	<0.001	−0.02	0.14

GA = geographic atrophy; GCC = ganglion cell layer complex, including ganglion cell body layer and inner plexiform layer; INL = inner nuclear layer; NFL = nerve fiber layer; OPL = outer plexiform layer; SD = standard deviation.

significantly reduced thickness in the photoreceptor layer and all-layer retina but no significant thickness change in NFL, GCC, INL, and OPL. In the non-GA region, photoreceptor thickness was significantly reduced, and there was no change in the other layers or all-layer retina.

DISCUSSION

THIS STUDY DEMONSTRATED A SIGNIFICANT DECREASE (9%–13% reduction) in retinal vessel densities in all 3 retinal plexi in GA eyes compared to age-matched normal controls subjects. The reduced retinal vessel density is likely associated with the significant loss of photoreceptors and ganglion cells as previously demonstrated in histopathologic studies of GA secondary to AMD. Kim and associates[10] studied 10 GA eyes and 5 normal control eyes histomorphometrically, demonstrating 76.9% ($P < 0.0001$) reduction of ONL cells and 30% ($P = 0.0008$) loss of ganglion cells in GA eyes compared to control eyes. Among GA eyes, the nuclei in all 3 layers were significantly reduced in segments in which the retinal pigment epithelium was completely absent.[10] The authors suggested trans-synaptic neuronal degeneration leads to secondary loss of ganglion cells due to chronically reduced input from photoreceptor loss. An experimental study in nonhuman primates demonstrated that macular focal laser induced RPE and photoreceptor destruction leads to subsequent retinal capillary closure 1 and 5 months later.[24] The current study used PR-OCTA to demonstrate in vivo retinal vessel density loss in all 3 retinal plexi, in addition to photoreceptor loss, in eyes with GA secondary to AMD.

An alternative explanation for the decrease of retinal vessel density in GA eyes is the potential increased oxygen flow from choroid to inner retina. The atrophy of RPE and photoreceptors, which normally consume large amounts of oxygen, could allow more of the oxygen from the choroid to diffuse to the inner half of the retina, which in turn could lead to a constriction of retinal vasculature. This is similar to the effect of panretinal photocoagulation on the inner retina.[25–27] However, one major difference is that choriocapillaris is compromised in GA eyes. It is unclear whether there could be increase of diffusion of oxygen to inner retina from the deeper choroidal vascular layers, which have been shown to rise to the level of Bruch's membrane in these eyes.[28]

The present findings of reduced photoreceptor thickness in GA are consistent with prior studies.[9,10] However, changes in inner retinal layer thickness were not found, which was reported in other studies. Using spectral-domain OCT with manual segmentations, Ramkumar and asscociates[9] found a 16% ganglion cell volume loss in GA eyes compared to age-matched controls eyes. Our methodology differed from this study. Because the reflectivity of the ganglion cell layer and that of IPL are similar, the authors were unable to reliably segment between these layers and reported the combined thickness of IPL and ganglion cell layers as the GCC; instead of reporting a separate ganglion cell layer thickness. Zucchiatti and associates[8] used spectral domain OCT (Cirrus HD-OCT, Zeiss) to automatically measure GCC in different stages of AMD patients, among whom 26 were GA patients. The authors found a significant 37% GCC loss in GA eyes compared to controls.[8] In that study there was no mention of manual segmentation and that may have resulted in segmentation errors. The automated segmentations in all 10 GA eyes in the present study were manually reviewed and adjusted to improve accuracy. Additional possible explanations for discrepancies include the fact that each study used different instruments, and study populations may have had variations. For example, eyes with greater duration of disease and larger areas of GA may have a greater degree of inner retinal degeneration.

Despite the nonsignificant inner retinal thickness change in GA eyes compared to normal control eyes, a significant

retinal vessel density decrease was found in all 3 plexi in GA eyes, suggesting vessel density measurement by OCTA may be more sensitive than structural thickness measurements for the detection of inner retinal changes in GA. One explanation for the paradoxical finding of a decrease in vessel density without decrease in thickness in inner retinal layers in GA region is that the inner retinal neurons were retained in this case, but their perfusion was reduced due to reduced metabolism from reduced synaptic activity secondary to loss of photoreceptors. Another possibility is that the inner retinal neurons were reduced in number, but the volume or thickness was made up by increased glial volume or extracellular matrix. It is also understandable that the biggest reduction happened in DCP among the 3 plexi in GA eyes, as the synaptic activity in the OPL should be reduced when there is photoreceptor atrophy.

Recent studies with using OCTA found significant impairment of choriocapillaris flow within the GA region and surrounding GA area, suggesting choriocapillaris blood flow alterations may be associated with the development and progression of GA.[23,29–35] Our study detected reduced retinal vessel density in all layers within GA. Interestingly, we noted reduced SVC and ICP in GA rim areas but not in DCP. A possible explanation for the reduced SCV and ICP but not DCP in the GA rim area is because ganglion cell in the rim have receptive fields that include photoreceptors in the GA region. This could theoretically result in reduced inner retinal metabolic demand in the GA rim area and subsequently reduced SVC and ICP blood flow. Because photoreceptors persist in the GA rim area, there is persistent metabolic demand for continued DCP blood flow. The lack of DCP reduction in the rim suggest that the reduction in retinal circulation might be a sequelae rather than a cause of GA. The fact that photoreceptor thickness is reduced in the rim suggests that photoreceptor atrophy could be part of the causal chain in GA and could be consistent with roles played by the RPE and choriocapillaris. Further study is needed to better understand the inner retinal blood flow in the pathogenesis of GA.

Currently, there is no treatment available for GA. Efforts to replace photoreceptors with stem cells or retinal prosthesis are under study. Given that only a 9%–13% reduction in retinal vessel density was found, even with significant loss of outer retinal photoreceptors in the atrophic area, there may be adequate inner retinal blood flow to support ganglion cell function following photoreceptor replacement or following stimulation by a retinal prosthesis. OCTA may reveal a useful biomarker to assess whether there is increased inner retinal blood flow changes following therapeutic intervention.

Limitations of the study include the cross-sectional design and a relatively small sample size. A longitudinal study with a larger sample size is needed to confirm our findings and to test whether the vessel density loss precedes retinal thinning. Despite the limitations, to the best of our knowledge, this is the first study on vessel density of three retinal capillary plexuses in GA eyes and may enrich the knowledge of natural history of GA.

In conclusion, quantifying vessel density using PR-OCTA demonstrated reduced perfusion in all three retinal plexi (SVC, ICP, and DCP) in eyes with GA compared to normal age-matched control eyes. Vessel density loss was greatest within regions of GA. OCTA-measured vessel density may be more sensitive than thickness measurement in detection of inner retinal changes in GA eyes.

Acknowledgements

ALL AUTHORS HAVE COMPLETED AND SUBMITTED THE ICMJE FORM FOR DISCLOSURE OF POTENTIAL CONFLICTS OF INTEREST and none were reported. Funding/support: Supported by US National Institutes of Health grants R01 EY024544, R01 EY027833, and P30 EY010572; by an unrestricted departmental funding grant; and by a William and Mary Greve Special Scholar Award from Research to Prevent Blindness. The funding sources had no role in the design and conduct of the study; collection, management, analysis, and interpretation of the data; preparation, review, or approval of the manuscript; and decision to submit the manuscript for publication. Financial disclosure: Drs. Jia and Huang have financial interests in Optovue. The other authors have indicated no financial support or financial conflict of interest.

REFERENCES

1. Flaxman SR, Bourne RRA, Resnikoff S, et al. Global causes of blindness and distance vision impairment 1990-2020: a systematic review and meta-analysis. *Lancet Glob Health* 2017;5:e1221–e1234.
2. Jonas JB, Cheung CMG, Panda-Jonas S. Updates on the epidemiology of age-related macular degeneration. *Asia Pac J Ophthalmol (Phila)* 2017;6:493–497.
3. Wong WL, Su X, Li X, et al. Global prevalence of age-related macular degeneration and disease burden projection for 2020 and 2040: a systematic review and meta-analysis. *Lancet Glob Health* 2014;2:e106–e116.
4. Holz FG, Strauss EC, Schmitz-Valckenberg S, van Lookeren Campagne M. Geographic atrophy: clinical features and potential therapeutic approaches. *Ophthalmology* 2014;121:1079–1091.
5. Brown DM, Kaiser PK, Michels M, et al. Ranibizumab versus verteporfin for neovascular age-related macular degeneration. *N Engl J Med* 2006;355:1432–1444.
6. Rosenfeld PJ, Brown DM, Heier JS, et al. Ranibizumab for neovascular age-related macular degeneration. *N Engl J Med* 2006;355:1419–1431.
7. Martin DF, Maguire MG, Ying GS, Grunwald JE, Fine SL, Jaffe GJ. Ranibizumab and bevacizumab for neovascular age-related macular degeneration. *N Engl J Med* 2011;364:1897–1908.

8. Zucchiatti I, Parodi MB, Pierro L, et al. Macular ganglion cell complex and retinal nerve fiber layer comparison in different stages of age-related macular degeneration. *Am J Ophthalmol* 2015;160:602–607.
9. Ramkumar HL, Nguyen B, Bartsch DU, et al. Reduced ganglion cell volume on optical coherence tomography in patients with geographic atrophy. *Retina* 2018;38:2159–2167.
10. Kim SY, Sadda S, Humayun MS, de Juan E Jr, Melia BM, Green WR. Morphometric analysis of the macula in eyes with geographic atrophy due to age-related macular degeneration. *Retina* 2002;22:464–470.
11. Spaide RF, Fujimoto JG, Waheed NK. Image artifacts in optical coherence tomography angiography. *Retina* 2015;35:2163–2180.
12. Wang J, Zhang M, Hwang TS, et al. Reflectance-based projection-resolved optical coherence tomography angiography [invited]. *Biomed Opt Express* 2017;8:1536–1548.
13. Zhang M, Hwang TS, Campbell JP, et al. Projection-resolved optical coherence tomographic angiography. *Biomed Opt Express* 2016;7:816–828.
14. Campbell JP, Zhang M, Hwang TS, et al. Detailed vascular anatomy of the human retina by projection-resolved optical coherence tomography angiography. *Sci Rep* 2017;7:42201.
15. Jia Y, Tan O, Tokayer J, et al. Split-spectrum amplitude-decorrelation angiography with optical coherence tomography. *Opt Express* 2012;20:4710–4725.
16. Zhang M, Wang J, Pechauer AD, et al. Advanced image processing for optical coherence tomographic angiography of macular diseases. *Biomed Opt Express* 2015;6:4661–4675.
17. Guo Y, Camino A, Zhang M, et al. Automated segmentation of retinal layer boundaries and capillary plexuses in wide-field optical coherence tomographic angiography. *Biomed Opt Express* 2018;9:4429–4442.
18. Gao SS, Jia Y, Liu L, et al. Compensation for reflectance variation in vessel density quantification by optical coherence tomography angiography. *Invest Ophthalmol Vis Sci* 2016;57:4485–4492.
19. Wei E, Jia Y, Tan O, et al. Parafoveal retinal vascular response to pattern visual stimulation assessed with OCT angiography. *PLoS One* 2013;8:e81343.
20. Zang P, Liu G, Zhang M, et al. Automated motion correction using parallel-strip registration for wide-field en face OCT angiogram. *Biomed Opt Express* 2016;7:2823–2836.
21. Hwang TS, Gao SS, Liu L, et al. Automated quantification of capillary nonperfusion using optical coherence tomography angiography in diabetic retinopathy. *JAMA Ophthalmol* 2016;134:367–373.
22. Hwang TS, Hagag AM, Wang J, et al. Automated quantification of nonperfusion areas in 3 vascular plexuses with optical coherence tomography angiography in eyes of patients with diabetes. *JAMA Ophthalmol* 2018;136:929–936.
23. Nassisi M, Shi Y, Fan W, et al. Choriocapillaris impairment around the atrophic lesions in patients with geographic atrophy: a swept-source optical coherence tomography angiography study. *Br J Ophthalmol* 2019;103:911–917.
24. Wilson DJ, Finkelstein D, Quigley HA, Green WR. Macular grid photocoagulation. An experimental study on the primate retina. *Arch Ophthalmol* 1988;106:100–105.
25. Budzynski E, Smith JH, Bryar P, Birol G, Linsenmeier RA. Effects of photocoagulation on intraretinal PO_2 in cat. *Invest Ophthalmol Vis Sci* 2008;49:380–389.
26. Grunwald JE, Riva CE, Brucker AJ, Sinclair SH, Petrig BL. Effect of panretinal photocoagulation on retinal blood flow in proliferative diabetic retinopathy. *Ophthalmology* 1986;93:590–595.
27. Feke GT, Green GJ, Goger DG, McMeel JW. Laser Doppler measurements of the effect of panretinal photocoagulation on retinal blood flow. *Ophthalmology* 1982;89:757–762.
28. Nesper PL, Lutty GA, Fawzi AA. Residual choroidal vessels in atrophy can masquerade as choroidal neovascularization on optical coherence tomography angiography: introducing a clinical and software approach. *Retina* 2018;38:1289–1300.
29. Choi W, Moult EM, Waheed NK, et al. Ultrahigh-speed, swept-source optical coherence tomography angiography in nonexudative age-related macular degeneration with geographic atrophy. *Ophthalmology* 2015;122:2532–2544.
30. Dansingani KK, Freund KB. Optical coherence tomography angiography reveals mature, tangled vascular networks in eyes with neovascular age-related macular degeneration showing resistance to geographic atrophy. *Ophthalmic Surg Lasers Imaging Retina* 2015;46:907–912.
31. Kvanta A, Casselholm de Salles M, Amren U, Bartuma H. Optical coherence tomography angiography of the foveal microvasculature in geographic atrophy. *Retina* 2017;37:936–942.
32. Moult EM, Waheed NK, Novais EA, et al. Swept-source optical coherence tomography angiography reveals choriocapillaris alterations in eyes with nascent geographic atrophy and drusen-associated geographic atrophy. *Retina* 2016;36(Suppl 1):s2–s11.
33. Sacconi R, Corbelli E, Carnevali A, Querques L, Bandello F, Querques G. Optical coherence tomography angiography in geographic atrophy. *Retina* 2018;38:2350–2355.
34. Waheed NK, Moult EM, Fujimoto JG, Rosenfeld PJ. Optical coherence tomography angiography of dry age-related macular degeneration. *Dev Ophthalmol* 2016;56:91–100.
35. Corbelli E, Sacconi R, Rabiolo A, et al. Optical coherence tomography angiography in the evaluation of geographic atrophy area extension. *Invest Ophthalmol Vis Sci* 2017;58:5201–5208.